

# Microscopic Insights into Extraction Mechanism of Copper(II) in Ammoniacal Solutions Studied by X-ray Absorption Spectroscopy and Density Functional Theory Calculation

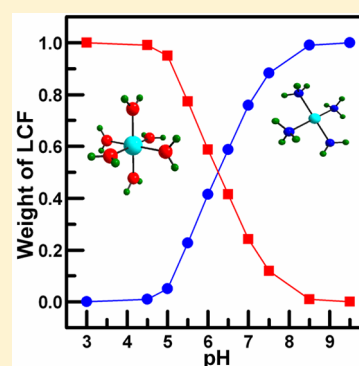
Jiugang Hu,<sup>†,‡,\*</sup> Qiyan Chen,<sup>†,‡</sup> Huiping Hu,<sup>†,‡</sup> Zheng Jiang,<sup>§</sup> Duo Wang,<sup>†</sup> Shubin Wang,<sup>†</sup> and Yaomin Li<sup>†</sup>

<sup>†</sup>College of Chemistry and Chemical Engineering, Central South University, Changsha 410083, China.

<sup>‡</sup>Key Laboratory of Resources Chemistry of Nonferrous Metals, Ministry of Education, Central South University, Changsha 410083, China

<sup>§</sup>Shanghai Synchrotron Radiation Facility, Shanghai Institute of Applied Physics, Chinese Academy of Sciences, Shanghai 201204, China

**ABSTRACT:** A microscopic investigation on the extraction process of copper(II) in ammoniacal solutions has been performed by X-ray absorption spectroscopy (XAS) and density functional theory (DFT) calculation. The structural change of copper(II) species in ammoniacal solution has been derived from X-ray absorption near-edge spectroscopy (XANES) by principal component analysis and linear combination fitting. It was found that the coordination structure of the extracted copper complex in the organic phases is planar square and independent of the aqueous pH, whereas the geometries of copper(II) species in ammoniacal solutions changed from axially elongated octahedron to distorted planar square with increase of pH. The coordination geometry and structural parameters of copper(II) species were further obtained by extended X-ray absorption fine structure (EXAFS) fitting and DFT calculation with the B3LYP functional. These results reveal that the formation of tetracoordinated copper(II) ammine species can evidently inhibit the copper extraction reaction. Thus, the extraction mechanism of copper(II) in ammoniacal solutions has been elucidated in view of the microscopic structural aspects of copper species in both organic phase and ammoniacal solutions.



## 1. INTRODUCTION

The separation and recovery of copper by solvent extraction technology is widely accepted in the fields of hydrometallurgy and environmental protection due to its advantages of energy-saving, ease in scale-up, and high efficiency. In recent years, solvent extraction of copper(II) in ammoniacal solutions has received great interest because a large number of low grade copper oxide ores and wastes have been extracted with ammonia leaching.<sup>1–3</sup> Moreover, wet etching of printed circuit boards and recycling of waste printed circuit boards using ammonia/ammonium salts have been put into practice for many years.<sup>4</sup> In our previous work,<sup>1</sup> it was found that the extraction percentage of copper(II) in ammoniacal solutions decreases when pH > 6.5. This phenomenon is unfavorable for the practical application of solvent extraction. In ammoniacal solutions, hydrated copper(II) can react with ammonia to form several copper(II) ammine species.<sup>5</sup> During the extraction process, the coordinated water and ammonia molecules of copper(II) species were replaced by hydrophobic ligands to realize the transfer of copper(II) from aqueous phase into organic phase. Thus, the coordination modes of copper species in both aqueous and organic phases can notably influence their reactivity and extraction efficiency.

Because of its d<sup>9</sup> electron configuration, copper(II) in solutions can form various geometries with a coordination number of 4, 5, or 6. The coordination structure of hydrated copper(II) and ammonia-coordinated copper(II) in aqueous solutions has been characterized by X-ray diffraction,<sup>6</sup> neutron diffraction,<sup>7</sup> X-ray absorption spectroscopy (XAS),<sup>8–11</sup> and quantum chemical methods.<sup>12,13</sup> However, it is more difficult for copper(II) to determine accurately the geometry than other metal ions because of its special Jahn–Teller effect. In the case of hydrated copper(II), although it is well-known that most of hydrated transition metal ions have a regular octahedral configuration, there is still an argument for coordination configuration of hydrated copper(II) so far. Various structural models for copper(II) have been proposed by different researchers, such as distorted octahedral geometry,<sup>8</sup> square pyramidal, trigonal bipyramidal, and planar-square configurations.<sup>7,9</sup> In 2001, Pasquarello et al. first reported that hydrated copper(II) is a trigonal bipyramidal configuration by the methods of neutron diffraction and first-principles molecular dynamics.<sup>7</sup> On the basis of the results of X-ray absorption near

Received: May 15, 2013

Revised: October 10, 2013

Published: November 5, 2013

edge spectroscopy (XANES) studies and ab initio calculations, Chaboy et al. proposed a dynamical model and thought that there is not a clearly preferred structure among those including four-, five-, and six-fold coordinated copper(II) ions but a structural exchange among themselves.<sup>9</sup> However, it is generally assumed that hydrated copper(II) has an axially elongated octahedral geometry. In ammoniacal solutions, the distribution of copper species dynamically changes with aqueous pH. To date, however, there has still not been the investigation of the coordination structure of multiple copper(II) species in ammoniacal solutions. The present theoretical and experimental studies only focus on the copper(II) species in solutions at a specific pH value. Benfatto et al. studied the coordination structure of  $\text{Cu}(\text{ClO}_4)_2$  in perchloric acid and 4 M aqueous ammonia by XANES and extended X-ray absorption fine structure (EXAFS) and thought that both  $\text{Cu}(\text{H}_2\text{O})_5^{2+}$  and  $\text{Cu}(\text{NH}_3)_5^{2+}$  are the trigonal bipyramidal configuration.<sup>10,11</sup> Rode et al. studied the structure of single-ammine copper(II) species by hybrid QM/MM MD simulation method at ab initio Hartree–Fock level.<sup>12,13</sup> The information obtained is very limited for elucidation of the extraction process of Cu(II) in ammoniacal solutions. Moreover, some reports showed that water and ammonia molecules could be coextracted into the organic phase.<sup>1,14</sup> Thus, the coordination state of the extracted complexes can also influence their distribution behavior. Therefore, a comprehensive understanding of coordination structure of dominant copper species in both ammoniacal solutions and the extracted organic phase is crucial to elucidate extraction mechanism and improve extractant formula.<sup>15,16</sup>

Synchrotron radiation X-ray absorption spectroscopy, including X-ray absorption near edge structure, and extended X-ray absorption fine structure, is a powerful approach to determine the microscopic structure of species in solutions.<sup>17</sup> In this work, the coordination structures of copper species in both ammoniacal solutions and the extracted organic phase were characterized by use of XAS. The XANES spectra can be used as a “fingerprint” to provide qualitative structural information of an unknown sample;<sup>18</sup> therefore, they were analyzed by principal component analysis (PCA) and linear components fitting (LCF) to clarify the effect of aqueous pH on the coordination modes of copper(II) species in ammoniacal solutions. The coordination geometry and structural parameters of copper(II) species were then obtained on the basis of the results of EXAFS spectra and density functional theory (DFT) calculation. Thus, the extraction mechanism of copper(II) in ammoniacal solutions has been elucidated in view of the microscopic structural aspects of copper species.

## 2. EXPERIMENTS

**2.1. Sample Preparation.** Ammoniacal copper solutions of varied pH were prepared by dissolving 0.02 mol/L copper sulfate and 1.0 mol/L ammonium sulfate in ultrapure water (Millipore Milli-Q System, 18.2 M $\Omega$  cm). The desired pH was adjusted by sodium hydroxide and sulfuric acid. As in the previous procedure,<sup>1</sup> the extracted copper complexes in the organic phases were prepared by solvent extraction from ammoniacal solution of pH 5.5, 7.5, and 9.5 with 0.2 mol/L 4-ethyl-1-phenyl-1,3-octadione in nonane, respectively.

**2.2. X-ray Absorption Measurements.** X-ray absorption spectra at the Cu K-edge of prepared samples were collected at the BL14W Beamline at Shanghai Synchrotron Radiation Facility (SSRF), China. The storage ring was operated at an energy of 3.5 GeV with a current between 150 and 210 mA.

All of the samples were measured in fluorescence mode using a silicon drift fluorescence detector at room temperature. A Si(111) double crystal monochromator was used for energy selection. The photon energy was calibrated against the first inflection point of the K-edge spectrum of copper foil to 8979.0 eV.

**2.3. XANES and EXAFS Analysis.** XAS data processing and analysis were performed using the ATHENA program in the IFEFFIT package following standard procedures.<sup>19</sup> All fits to the extended X-ray absorption fine structure (EXAFS) data were performed using the ARTEMIS program. Because X-ray absorption spectra are a statistically weighted average for all species in solution, the normalized XANES spectra of copper species in ammoniacal solutions were analyzed with a three-step procedure:<sup>15</sup> (i) decomposition of the experimental spectra into principal components using factor analysis (PCA) in combination with target transformation by SIXpack program;<sup>20</sup> (ii) quantification of identified species in each unknown sample by the linear combination fit (LCF) method using the program ATHENA;<sup>21</sup> (iii) standard shell fitting of EXAFS spectra to gain structural parameters of the limiting structural units. The EXAFS oscillations were extracted from normalized XAS spectra and weighted by  $k^3$  to enhance the magnitude. For each fitting, the amplitude reduction factor ( $S_0^2$ ) is fixed at 0.85. The bond length ( $r$ ) and the Debye–Waller factor ( $\sigma^2$ ) were allowed to vary. A single threshold energy shift ( $\Delta E_0$ ) was also varied and constrained to the same value for all paths. Theoretical backscattering amplitude and phase-shift functions were generated from the crystal structure of model compounds with FEFF 7.02,<sup>22</sup> i.e.,  $\text{Cu}(\text{H}_2\text{O})_6(\text{ClO}_4)_2$  and  $\text{Cu}(\text{NH}_3)_4(\text{NO}_3)_2$  for copper(II) species in ammoniacal solutions and copper(II) acetylacetonate complex for copper extracts in organic phases. Single scattering paths for EXAFS fitting include the contribution of coordinated oxygen/nitrogen atoms for copper(II) species in ammoniacal solutions, whereas the contribution of both coordinated oxygen atoms and noncoordinated carbon atoms were considered for copper extracts in the organic phases.

**2.4. DFT Calculation Details.** All calculations were carried out with the Gaussian 03 program<sup>23</sup> at the high performance computing center of Central South University. The geometric configuration of copper(II) species was optimized in the gas phase using the B3LYP hybrid exchange–correlation functional, viz., Becke’s three-parameter exchange functional (B)<sup>24</sup> and the Lee–Yang–Parr correlation (LYP) functional,<sup>25</sup> and a 6-31G(d) basis set for all atoms. No relativistic effect was considered. The optimized geometries were checked by frequency analysis at the same level of theory to ensure the energy-minimized geometry for each complex. Single point energy calculations of the optimized geometries were performed on the basis set of B3LYP/6-311+G(d,p). The enthalpy difference of copper(II) species was calculated using the following equation:  $\Delta E = E_{\text{Cu}(\text{NH}_3)_x(\text{H}_2\text{O})_y^{2+}} - E_{\text{Cu}^{2+}} - xE_{\text{NH}_3} - yE_{\text{H}_2\text{O}}$  ( $x + y = 4$  or  $6$ ).

## 3. RESULTS AND DISCUSSION

**3.1. XAS of Copper Extracts.** The normalized Cu K-edge XANES spectra of copper extracts in organic phases are shown in Figure 1. Under three different pH conditions, the extracted copper complexes exhibit the same spectral signature, indicating that a pH change of aqueous phase does not influence the coordination structure of copper extracts. It was clearly

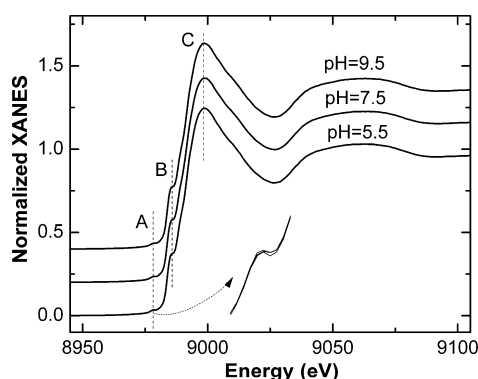


Figure 1. Normalized Cu K-edge XANES spectra of copper extracts.

observed that a strong white line peak (C) appears at around 8998 eV, which is attributed to the  $1s \rightarrow 4p_{x^2-y^2}$  transition in copper complexes. The weak pre-edge absorption peak at 8978 eV (A) is assigned to the  $1s \rightarrow 3d$  electronic transition due to the dipole-forbidden copper complexes. Moreover, the appearance of shoulder peak B at 8985 eV indicates that the configuration of copper extracts in organic phases is plane square because the electron of s-orbital can migrate to the z-direction of the p-orbital with an empty state ( $1s \rightarrow 4p_z$ ). Similar spectral signatures were also observed for copper complexes with the plane square configuration.<sup>26</sup> From these symmetry indications, the structural sketch of copper extracts drawn in Figure 2 may be supposed.

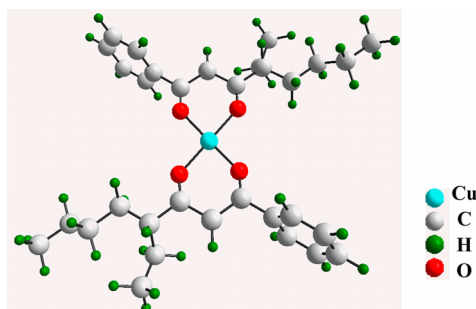


Figure 2. Probable structural sketch of copper extracts.

The  $k^3$ -weighted Cu K-edge EXAFS spectra of copper extracts in organic phases and their corresponding Fourier transforms are shown in Figure 3. There is no distinct difference among these peaks in Fourier transforms, indicating that copper extracts have similar coordination structures under different pH conditions. The first strong peak at ca. 1.53 Å (phase shifts are not corrected) corresponds to the first coordination shell of copper extracts, which should include the contributions from the coordinated oxygen atoms of  $\beta$ -diketone ligands. During the fitting process, copper(II) acetylacetonate was used as the model compound. Four kinds of scattering paths were shown in Figure 4. It was found that the fitting result is unreasonable unless including the contribution of the multiple scattering path of  $\text{Cu} \rightarrow \text{C1} \rightarrow \text{O}$ . Thus, three kinds of single scattering paths ( $\text{Cu} \rightarrow \text{O}$ ,  $\text{Cu} \rightarrow \text{C1}$ ,  $\text{Cu} \rightarrow \text{C2}$ ) and a multiple scattering path of  $\text{Cu} \rightarrow \text{C1} \rightarrow \text{O}$  were considered for EXAFS fitting of copper extracts. Because it is well-known that the stoichiometric ratio of Cu(II) with  $\beta$ -diketone ligands is 1:2, the number of fitting paths was fixed at four for Cu–O and Cu–C1, Cu–C1–O and two for Cu–C2, respectively. The best fitting results are

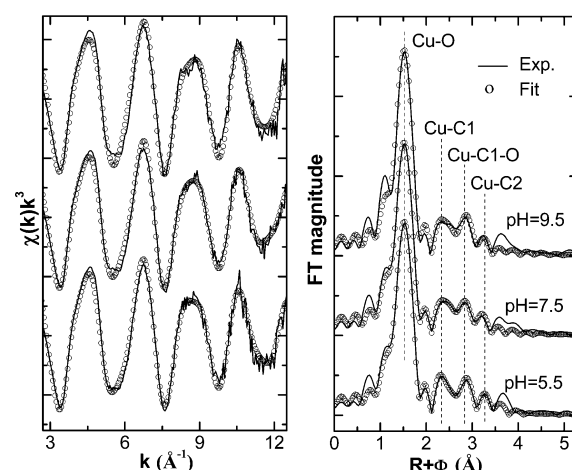


Figure 3. Cu K edge  $k^3$ -weighted EXAFS (left) and their Fourier transforms (right) of copper extracts in organic phase.

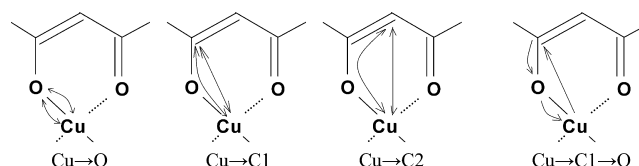


Figure 4. Scattering paths of copper extracts for EXAFS fitting.

collected in Table 1. There is no distinct difference on the parameters for inner-sphere coordination of copper extracts. The mean distance of Cu–O is ca. 1.97 Å. Therefore, when copper(II) was extracted from ammoniacal solutions with  $\beta$ -diketone, the configuration of copper extracts is plane square and is independent of pH of ammoniacal solutions.

**3.2. XAS of Cu(II) Species in Ammoniacal Solutions.** In ammoniacal solutions, several copper(II) species simultaneously exist because ammonia molecule replaces successively the coordinated water molecules of hydrated copper(II) to form various copper(II) ammine complexes with increasing pH. Although copper(II) species in ammoniacal solutions have been widely studied by traditional UV–vis spectroscopy<sup>27,28</sup> and potentiometric titration,<sup>29</sup> these methods are hardly exploitable to elucidate the microscopic structure change of copper(II). X-ray absorption spectroscopy is one of the best methods to determine the coordination structure of species in solutions. It is worth noting that it is almost impossible to distinguish the contribution of O and N atoms using XAS because of their close Z number and similar amplitudes and phase functions. However, as shown in Figure 5, it can be found that the normalized XANES spectra of copper(II) species in ammoniacal solutions exhibit evident differences with increasing pH, including sharpness, position, and intensity.

All spectra present a weak pre-edge peak (A) at 8978 eV, which results from the  $1s \rightarrow 3d$  electron transition. Meanwhile, two distinct features can be observed in the series of XANES spectra. On one hand, a symmetric white line peak (B,  $1s \rightarrow 4p$  transition) can be found at pH < 5.0, indicating the octahedral configuration for hydrated copper(II). The results agree with that derived by Persson.<sup>8</sup> On the other hand, XANES spectra broaden and present a weak shoulder at ca. 9000 eV when the pH is larger than 5.0. The white line peak exhibits a pronounced splitting (B and B') at pH > 6.0. These spectral changes can be assigned to the geometry change of copper(II) species due to more steric hindrance of ammonia than water. Moreover,

Table 1. Best Fitting Parameters of EXAFS Spectra of Copper Extracts in Organic Phases<sup>a</sup>

sample	shell	$N^{b,g}$	$r^c$	$\sigma^2 (\times 10^{-3})^d$	$\Delta E_0^e$	$R\%^f$
pH = 5.5	Cu–O	4	1.97 (1)	3.8 (1)	4.2 (5)	5.9
	Cu–C1	4	2.84 (2)	5.6 (5)	6.7 (3)	
	Cu–C2	2	3.62 (2)	3.3 (4)		
pH = 7.5	Cu–O	4	1.97 (1)	3.8 (7)	4.2 (5)	6.2
	Cu–C1	4	2.85 (2)	5.2 (3)	7.2 (4)	
	Cu–C2	2	3.64 (2)	11.3 (2)		
pH = 9.5	Cu–O	4	1.96 (2)	3.3 (7)	4.5 (6)	10.7
	Cu–C1	4	2.85 (2)	3.1 (2)	7.5 (2)	
	Cu–C2	2	3.64 (2)	6.7 (5)		

<sup>a</sup>Fitting range:  $\Delta k = 2.7\text{--}12.2 \text{ \AA}^{-1}$ ,  $\Delta R = 1.0\text{--}3.5 \text{ \AA}$ . Values in parentheses are statistical uncertainties. <sup>b</sup>Coordination number. <sup>c</sup>Bond distance ( $\text{\AA}$ ). <sup>d</sup>Debye–Waller factor ( $\text{\AA}^2$ ). <sup>e</sup>Threshold energy shift (eV). <sup>f</sup>R-factor. <sup>g</sup>Fixed parameters.

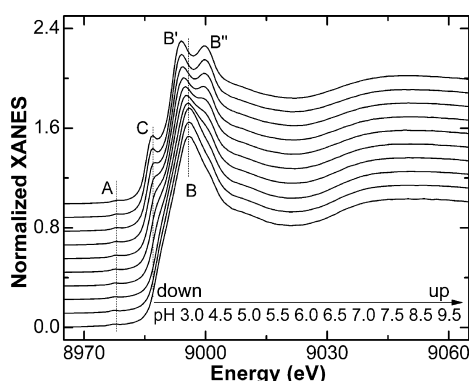


Figure 5. Normalized Cu K-edge XANES spectroscopy of copper(II) species.

the coordination number of hydrated copper(II) species could decrease when coordinated water molecules are replaced by ammonia. The results indicate that the coordination of copper(II) with ammonia weakens the scattering resonances, thus decreasing the intensity of white-line. The presence of a new absorption peak (C) at 8987 eV, which can be attributed to  $1s \rightarrow 4p_z$  transition and shakedown contributions, clearly indicates the planar square configuration of copper(II) species.<sup>28</sup> The results are in line with the XANES analysis of  $\text{Cu}(\text{NH}_3)_4^{2+}$  reported by Chaboy.<sup>30</sup>

Because all of the copper(II) species in ammoniacal solution can contribute to the weighted XAS spectra, it is difficult to extract the structure information of the individual species by conventional EXAFS fitting. However, the XANES spectra can

be used as a “fingerprint” to provide qualitative structural information of an unknown sample.<sup>18</sup> Furthermore, the close Z number and similar amplitudes and phase functions of O and N atoms indicate that the XANES spectral change of copper(II) species could mainly result from their configuration change. Thus, on the basis of the spectral additivity, XANES spectra can be analyzed by PCA and LCF to clarify the effect of aqueous pH on the coordination modes of copper(II) species in ammoniacal solutions.<sup>31,32</sup> As shown in Figure 6a, the PCA results show that two principal configurations can be statistically distinguished. One factor could be the octahedral structure and the other could be the planar square structure. The target transformation analysis shows that experimental and reproduced spectra on Figure 6b are almost superimposed, indicating that the predominant configuration of copper(II) species in solutions can be represented by these two limiting structural units. Although there are probably copper(II) species with mixed coordination of water and ammonia in solutions, it is difficult to derive them from XANES spectra due to their spectral similarity with the limiting structural units.

Least combination fitting was performed for XANES spectra using the spectra at pH 3.0 and 9.5 as possible end members to obtain the quantitative information of principal components in each sample. As shown in Figure 7, the relative content of the octahedral structural unit in solutions decreases with the increase of pH. Accordingly, the content of the square-planar structure unit increases. Especially, when one ammonia molecule coordinates with hexahydrated  $\text{Cu}(\text{II})$ , the geometry of copper(II) species still keeps octahedral configuration, whereas the coordination configuration of copper(II) species

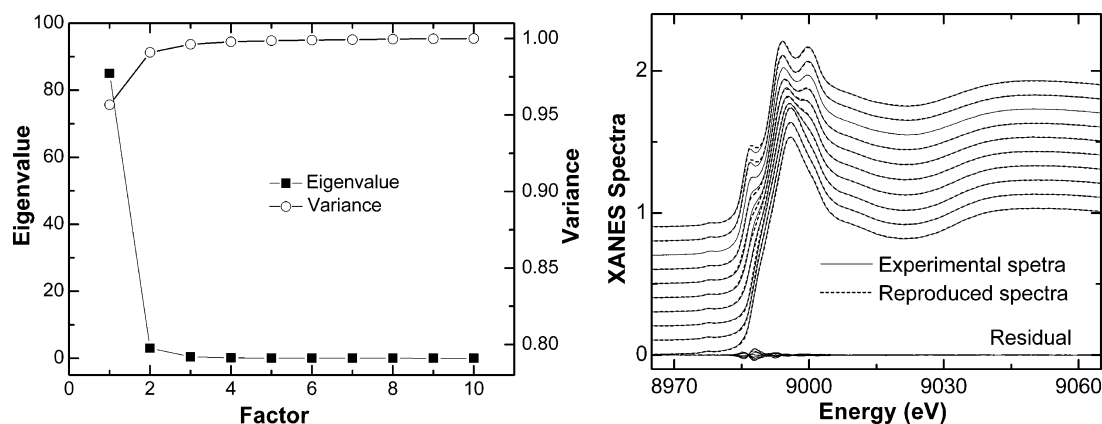


Figure 6. (a) Principal component analysis of XANES spectra of copper(II) species. (b) Target transformation of normalized XANES spectra.



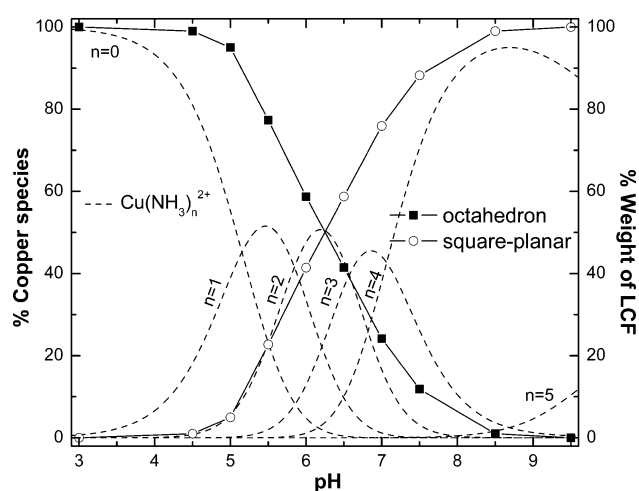


Figure 7. Distribution of principal components as a function of pH.

changes from octahedron to planar square when the water of hydrated copper(II) is replaced with two and more ammonia molecules. These results are consistent with the theoretical investigations,<sup>33,34</sup> indicating that the introduction of  $\text{NH}_3$  ligands increases the stability of hydrated copper(II). As a consequence, an undesirable decrease trend on the extraction efficiency of Cu(II) at  $\text{pH} > 6.5$  can be attributed to the formation of more stable copper(II) ammine species.

On the basis of the previous results, the local atomic environment of Cu(II) in ammoniacal solutions was further investigated with EXAFS fitting by using  $\text{Cu}(\text{H}_2\text{O})_6(\text{NO}_3)_2$  for pHs 3.0 and 5.5 and  $\text{Cu}(\text{NH}_3)_4(\text{ClO}_4)$  for pHs 7.5 and 9.5 as the model compounds, respectively. Taking into consideration the Jahn–Teller effect of copper(II), EXAFS fitting was performed with a two shell model. The results are shown in Figure 8 and Table 2. A strong FT peak for pHs 3.0 and

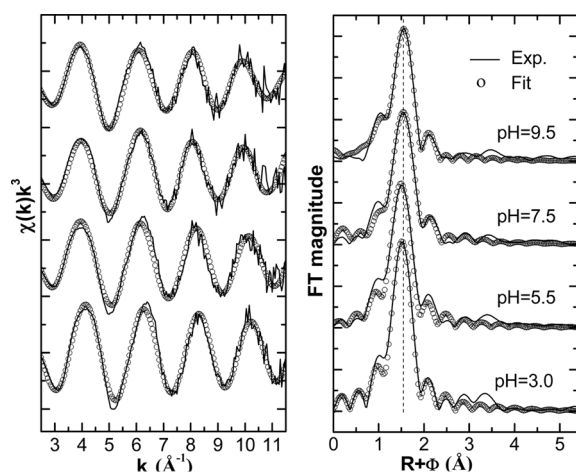


Figure 8. Cu K edge  $k^3$ -weighted EXAFS (left) and their Fourier transforms (right) of copper(II) species.

9.5 appeared at 1.51 and 1.54 Å, respectively, which corresponds to the contribution of Cu–O of hydrated copper(II) and Cu–N of copper(II) ammine species. For hexahydrated copper(II) at pH 3.0, the respective bond length of equatorial Cu–O and axial Cu–O is 1.96 Å and 2.28 Å, which indicates a distorted octahedral configuration of hexahydrated copper(II).<sup>8</sup> Moreover, the Cu–O<sub>eq</sub> bond length of copper(II) species at pH 5.5

Table 2. Best Fitting Parameters of EXAFS Spectra of Copper Species in the Aqueous Phase<sup>a</sup>

sample	shell	$N^{b,g}$	$r^c$	$(\sigma^2 \times 10^{-3})^{d,f}$	$\Delta E_0^e$	$R\%^f$
pH = 3.0	Cu–O <sub>eq</sub>	4	1.96 (1)	2.4 (4)	2.4 (3)	1.8
	Cu–O <sub>ax</sub>	2	2.28 (2)	7.1 (8)		
pH = 5.5	Cu–O <sub>eq</sub>	4	1.98 (2)	4.5 (3)	1.7 (5)	5.7
	Cu–O <sub>ax</sub>	2	2.25 (2)	8.7 (5)		
pH = 7.5	Cu–N <sub>eq</sub>	2	2.00 (1)	6.8 (4)	7.4 (6)	7.1
	Cu–N <sub>eq</sub>	2	2.02 (2)	9.2 (4)		
pH = 9.5	Cu–N <sub>eq</sub>	2	2.01 (2)	4.3 (7)	3.5 (2)	3.5
	Cu–N <sub>eq</sub>	2	2.02 (1)	6.5 (6)		

<sup>a</sup>Fitting range:  $\Delta k = 2.5\text{--}11.5 \text{ \AA}^{-1}$ ,  $\Delta R = 1.0\text{--}2.5 \text{ \AA}$ . Values in parentheses are statistical uncertainties. <sup>b</sup>Coordination number. <sup>c</sup>Bond distance (Å). <sup>d</sup>Debye–Waller factor ( $\text{\AA}^2$ ). <sup>e</sup>Threshold energy shift (eV). <sup>f</sup>R-factor. <sup>g</sup>Fixed parameters.

increases to 1.98 Å, accompanying that the Cu–O<sub>ax</sub> bond length decreases to 2.25 Å. Due to the configuration change, the bond length of Cu–N is about 2.01 and 2.02 Å for copper(II) ammine species at pHs 7.5 and 9.5. Although some studies suggest the configuration of tetraammine Cu(II) is planar-square,<sup>9</sup> due to the Jahn–Teller effect of copper(II) and steric hindrance of ammonia molecule, the decrease of symmetry of the  $p_x^2 - y^2$  orbital plane of copper(II) ammine species results in the typical splitting feature of XANES spectra, indicating a quasi-tetrahedral configuration for tetraammine copper(II). Thus, copper(II) coordinates with four ammonia molecules to form a distorted plane-square configuration. Compared with the case of tetraamminecopper(II), the XANES feature of the extracted copper complexes in organic phases is evidently different because of the chelate effect and conjugation effect of  $\beta$ -diketone ligands. This phenomenon was also reported for the structure of other tetracoordinated copper species.<sup>26</sup> For instance, Chaboy et al. investigated the coordination structure of four nitrogen-containing ligands (ammonia, ethylenediamine, phthalocyanine, and glycine) with copper(II) by X-ray absorption spectroscopy. They found that although four copper species are tetracoordinated structure, their XANES features are evidently different, indicating the structure and property of ligands have pronounced effect on the geometry of coordinated ions.<sup>30</sup>

**3.3. DFT Calculation of Cu(II) Species.** The structure and energy of a series of conformers of  $[\text{Cu}(\text{NH}_3)_x(\text{H}_2\text{O})_y]^{2+}$  ( $x + y = 4$  or 6) in the gas phase were further calculated at the B3LYP level to analyze their stability and the dominant structure of copper(II) species in ammoniacal solution. Six energetically stable geometries are depicted in Figure 9, and their corresponding structural parameters are shown in Table 3. It was found that the configuration of hexahydrated copper(II) is the axially elongated octahedral geometry. The axial and planar bond length of Cu–O are 2.317 and 1.992 Å, respectively. A similar result for  $\text{Cu}(\text{H}_2\text{O})_6^{2+}$  was reported by Burda et al.<sup>35</sup> at the DFT level of theory with the B3PW91 functional. When only one ammonia molecule coordinates with Cu(II), the configuration of copper(II) species still keeps octahedral geometry. Because of the larger copper–ammonia binding energy and molecular volume of ammonia, the Cu–O<sub>ax</sub> bond length slightly decreases whereas the Cu–O<sub>eq</sub> bond length slightly increases. However, when two and more ammonia molecules coordinate with hydrated copper(II), the geometry of copper species changes from octacoordination to tetracoordination, accompanying the

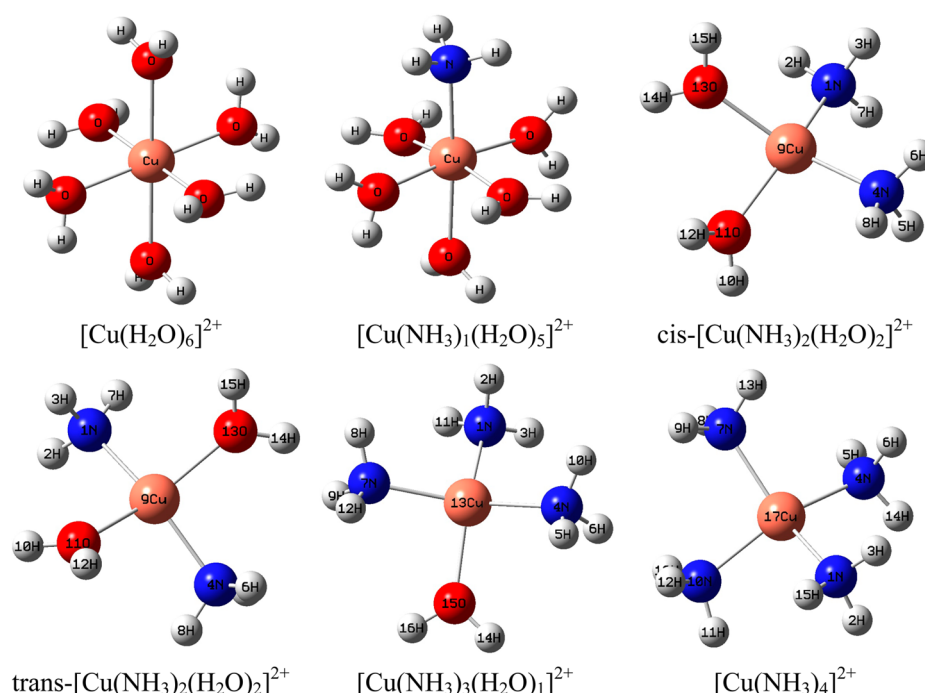


Figure 9. Optimum structures of copper(II) species.

Table 3. Structural Parameters of Copper(II) Species

species	mean bond length ( <i>d</i> , Å)	bond angle ( $\angle$ , deg)	
$[\text{Cu}(\text{H}_2\text{O})_6]^{2+}$	Cu–O <sub>ax</sub>	2.317	
	Cu–O <sub>eq</sub>	1.992	
$[\text{Cu}(\text{NH}_3)_1(\text{H}_2\text{O})_5]^{2+}$	Cu–N <sub>ax</sub>	2.251	
	Cu–O <sub>ax</sub>	2.293	
$\text{cis}-[\text{Cu}(\text{NH}_3)_2(\text{H}_2\text{O})_2]^{2+}$	Cu–O <sub>eq</sub>	2.003	
	Cu–N	1.992	4N–Cu–13O 148.39
$\text{trans}-[\text{Cu}(\text{NH}_3)_2(\text{H}_2\text{O})_2]^{2+}$	Cu–O	1.986	1N–Cu–11O 148.29
	Cu–N	1.992	4N–Cu–1N 154.21
$[\text{Cu}(\text{NH}_3)_3(\text{H}_2\text{O})_1]^{2+}$	Cu–O	1.987	11O–Cu–13O 142.85
	Cu–N	2.008	4N–Cu–7N 148.30
$[\text{Cu}(\text{NH}_3)_4]^{2+}$	Cu–O	2.006	1N–Cu–15O 143.31
	Cu–N	2.028	1N–Cu–7N 146.90

decrease of mean bond length of Cu–O and the increase of mean bond length of Cu–N. For both *trans*- and *cis*- $[\text{Cu}(\text{NH}_3)_2(\text{H}_2\text{O})_2]^{2+}$ , the average bond lengths of Cu–N and Cu–O are equal to 1.992 and 1.986 Å, respectively. The respective bond angle of  $\angle 1\text{N}-\text{Cu}-13\text{O}$  and  $\angle 11\text{O}-\text{Cu}-13\text{O}$  is  $148.39^\circ$  and  $148.29^\circ$  for the *cis*-configuration. However, the respective bond angle of  $\angle 1\text{N}-\text{Cu}-11\text{O}$  and  $\angle 4\text{N}-\text{Cu}-13\text{O}$  is  $154.21^\circ$  and  $142.85^\circ$  for *trans*-configuration. It was noteworthy that the mean bond length of Cu–N and bond angle of  $\angle 1\text{N}-\text{Cu}-7\text{N}$  of  $[\text{Cu}(\text{NH}_3)_4]^{2+}$  is 2.028 Å and  $146.9^\circ$ , respectively. The results indicate that tetracoordinated copper(II) ammine species in ammoniacal solutions present a distorted plane-square configuration. On the basis of *ab initio* dynamic simulations, a similar distortion of the planar square configuration of  $[\text{Cu}(\text{NH}_3)_4]^{2+}$  was reported by Berces et al.<sup>36</sup> Thus, the predominant configurations of copper(II) species in ammoniacal solutions are axially elongated octahedron and distorted plane-square, which is in accordance with the results of the previous XANES analysis.

The enthalpy difference for each copper(II) species is shown in Table 4. For the copper(II) species with the same

Table 4. Enthalpy Difference of Copper(II) Species ( $\Delta E$ , kcal/mol)

species	$\Delta E$ (kcal/mol)
$[\text{Cu}(\text{H}_2\text{O})_6]^{2+}$	–359.5
$[\text{Cu}(\text{NH}_3)_1(\text{H}_2\text{O})_5]^{2+}$	–373.5
$\text{cis}-[\text{Cu}(\text{NH}_3)_2(\text{H}_2\text{O})_2]^{2+}$	–343.8
$\text{trans}-[\text{Cu}(\text{NH}_3)_2(\text{H}_2\text{O})_2]^{2+}$	–342.2
$[\text{Cu}(\text{NH}_3)_3(\text{H}_2\text{O})_1]^{2+}$	–357.1
$[\text{Cu}(\text{NH}_3)_4]^{2+}$	–370.4

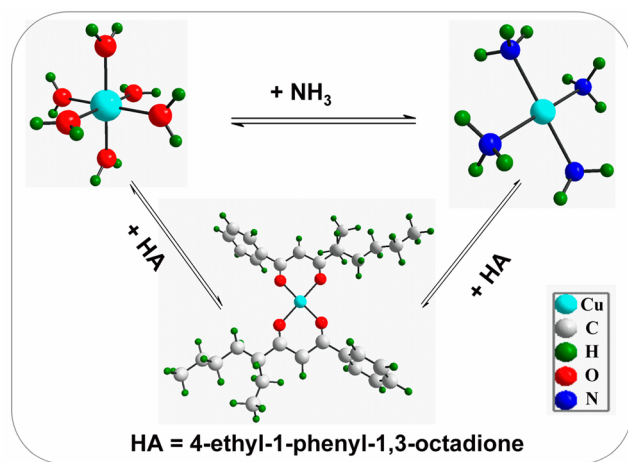
configuration, the results show that the enthalpy difference of hydrated copper(II) ammine species increases about 14 kcal/mol with an increase of coordinated ammonia. The enthalpy difference mainly results from, on the one hand, the configuration change of copper(II) species and, on the other hand, the larger mean bonding energy of Cu–N than Cu–O. The mean bonding energy evidently increases from the 59.9 kcal/mol for  $[\text{Cu}(\text{H}_2\text{O})_6]^{2+}$  to the 92.6 kcal/mol for  $[\text{Cu}(\text{NH}_3)_4]^{2+}$ . Thus, the stability increase of copper(II) species in ammoniacal solutions could result in the decrease of their reactivity.<sup>33,34</sup>

### 3.4. Microscopic Mechanism of Copper Extraction.

The coordination modes of copper species in both aqueous and organic phases play a significant role in the extraction of copper(II). On the basis of the discussion above, the coordination structure of the extracted copper complexes in organic phases is planar square and independent of the aqueous pH, whereas the geometry of copper(II) species in ammoniacal solutions changes from axially elongated octahedron to distorted planar square with the increase of pH. Although some studies indicated that only free Cu(II) in ammoniacal solutions can be extracted,<sup>37</sup> the results in our work certify that the copper(II) ammine species can be simultaneously extracted under the conditions of high pH or high ammonia concentration. Because the increase of stability of copper(II) ammine species inhibits the extraction reaction, the percentage

extraction of copper(II) decreases with the increase of copper(II) species with distorted planar square configuration in aqueous phase.<sup>1</sup> Thus, as shown in Scheme 1, a probable

**Scheme 1. Extraction Mechanism of Copper(II) in Ammoniacal Solution**



microscopic mechanism can be proposed for the solvent extraction of copper(II) in ammoniacal solutions.

#### 4. CONCLUSIONS

Coordination modes of copper species during the solvent extraction process can dramatically influence its distribution behavior. The present work presents a comprehensive understanding of the coordination structure of dominant copper species in both the extracted organic phase and ammoniacal solutions by X-ray absorption spectroscopy and DFT calculation. It was found that the configuration of the extracted copper complex in organic phases is planar square and independent of the aqueous pH. XANES results derived by PCA and LCF indicate that there are two kinds of dominant geometries for copper(II) species in the series of ammoniacal solutions, i.e., axially elongated octahedron and distorted planar square. When two and more ammonia molecules coordinate with hydrated copper(II) in ammoniacal solutions, the coordination number of copper(II) species decreases and their geometries change from axially elongated octahedron to distorted planar square, thus increasing their stability and decreasing their reactivity. The proposed structure models of copper(II) species based on the XANES and EXAFS were consistent with the results of DFT calculations. The decrease trend of percentage extraction of copper(II) in ammoniacal solutions at higher pH is mainly attributed to the formation of tetracoordinated copper(II) species with distorted planar-square configuration.

#### AUTHOR INFORMATION

##### Corresponding Author

\*J. Hu: e-mail, hjg.csu@gmail.com; tel, 86 731 88879616; fax, 86 731 88879616.

##### Notes

The authors declare no competing financial interest.

#### ACKNOWLEDGMENTS

We express our gratitude to beamline BL14W1 at Shanghai Synchrotron Radiation Facility for providing the beam time.

We also thank the anonymous reviewers for their valuable comments. This work was supported by the National Basic Research Program of China (No. 2014CB643401), National Natural Science Foundation of China (No. 51134007 and 51304244), and the Postdoctoral Science Foundation of Central South University.

#### REFERENCES

- (1) Hu, J.; Chen, Q.; Hu, H.; Chen, X.; Ma, Q.; Yin, Z. Extraction Behavior and Mechanism of Cu(II) in Ammoniacal Sulfate Solution with  $\beta$ -diketone. *Hydrometallurgy* **2012**, 127–128, 54–61.
- (2) Wieszczycka, K.; Kaczerewska, M.; Krupa, M.; Parus, A.; Olszanowski, A. Solvent Extraction of Copper(II) from Ammonium Chloride and Hydrochloric Acid Solutions with Hydrophobic Pyridineketoximes. *Sep. Purif. Technol.* **2012**, 95, 157–164.
- (3) Alguacil, F. J.; Alonso, M. Recovery of Copper from Ammoniacal/Ammonium Sulfate Medium by LIX 54. *J. Chem. Technol. Biotechnol.* **1999**, 74, 1171–1175.
- (4) Oishi, T.; Koyama, K.; Alam, S.; Tanaka, M.; Lee, J. C. Recovery of High Purity Copper Cathode from Printed Circuit Boards Using Ammoniacal Sulfate or Chloride Solutions. *Hydrometallurgy* **2007**, 89, 82–88.
- (5) Alguacil, F. J.; Sastre, A. M. Mechanistic Study of Active Transport of Copper (II) Using LIX 54 Across a Liquid Membrane. *J. Chem. Technol. Biotechnol.* **2000**, 75, 577–582.
- (6) Musinu, A.; Paschina, G.; Piccaluga, G.; Magini, M. Coordination of Copper(II) in Aqueous Copper Sulfate Solution. *Inorg. Chem.* **1983**, 22, 1184–1187.
- (7) Pasquarello, A.; Petri, I.; Salmon, P. S.; Parisel, O.; Car, R. First Solvation Shell of the Cu (II) Aqua Ion: Evidence for Fivefold Coordination. *Science* **2001**, 291, 856.
- (8) Persson, I.; Persson, P.; Sandstrom, M.; Ullstrom, A.-S. Structure of Jahn-Teller Distorted Solvated Copper(II) Ions in Solution, and in Solids with Apparently Regular Octahedral Coordination Geometry. *J. Chem. Soc., Dalton Trans.* **2002**, 1256–1265.
- (9) Chaboy, J.; Muñoz-Páez, A.; Merklings, P. J.; Marcos, E. S. The Hydration of Cu: Can the Jahn-Teller Effect be Detected in Liquid Solution? *J. Chem. Phys.* **2006**, 124, 1–10.
- (10) D'Angelo, P.; Benfatto, M.; Della Longa, S.; Pavel, N. Evidence of Distorted Fivefold Coordination of the Cu<sup>2+</sup> Aqua Ion from an X-ray Absorption Spectroscopy Quantitative Analysis. *Phys. Rev. B* **2002**, 66, 1–7.
- (11) Frank, P.; Benfatto, M.; Hedman, B.; Hodgson, K. O. Solution [Cu(amm)]<sup>2+</sup> is a Strongly Solvated Square Pyramid: A Full Account of the Copper K-edge XAS Spectrum Within Single-Electron Theory. *Inorg. Chem.* **2008**, 47, 4126–4139.
- (12) Schwenk, C. F.; Rode, B. M. The Influence of the Jahn-Teller Effect and of Heteroligands on the Reactivity of Cu<sup>2+</sup>. *Chem. Commun.* **2003**, 39, 1286–1287.
- (13) Schwenk, C. F.; Rode, B. M. Influence of Heteroligands on Structural and Dynamical Properties of Hydrated Cu<sup>2+</sup>: QM/MM MD Simulations. *Phys. Chem. Chem. Phys.* **2003**, 5, 3418–3427.
- (14) Flett, D.; Melling, J. Extraction of Ammonia by Diketone Extractants. *Hydrometallurgy* **1980**, 5, 283.
- (15) Hu, J.; Chen, Q.; Hu, H.; Chen, X.; Hu, F.; Yin, Z. XAS Investigation on the Coordination Structure and Extraction Mechanism of Zinc(II) in Ammoniacal Solution. *Sep. Purif. Technol.* **2012**, 98, 308–314.
- (16) Gannaz, B.; Antonio, M. R.; Chiarizia, R.; Hill, C.; Cote, G. Structural Study of Trivalent Lanthanide and Actinide Complexes Formed upon Solvent Extraction. *Dalton Trans.* **2006**, 4553–4562.
- (17) Denecke, M. A. Actinide Speciation Using X-ray Absorption Fine Structure Spectroscopy. *Coord. Chem. Rev.* **2006**, 250, 730–754.
- (18) Penner-Hahn, J. E. Characterization of “spectroscopically quiet” Metals in Biology. *Coord. Chem. Rev.* **2005**, 249, 161–177.
- (19) Ravel, B.; Newville, M. ATHENA, ARTEMIS, HEPHAESTUS: Data Analysis for X-ray Absorption Spectroscopy Using IFEFFIT. *J. Synchrotron. Radiat.* **2005**, 12, 537–541.

- (20) Webb, S. M. SIXpack: A Graphical User Interface for XAS Analysis Using IFEFFIT. *Phys. Scr.* **2005**, 1011.
- (21) Ressler, T.; Wong, J.; Roos, J.; Smith, I. L. Quantitative Speciation of Mn-bearing Particulates Emitted from Autos Burning (Methylcyclopentadienyl) Manganese Tricarbonyl-added Gasolines Using XANES Spectroscopy. *Environ. Sci. Technol.* **2000**, 34, 950–958.
- (22) Ankudinov, A.; Ravel, B.; Rehr, J.; Conradson, S. Real-space Multiple-scattering Calculation and Interpretation of X-ray Absorption Near Edge Structure. *Phys. Rev. B* **1998**, 58, 7565.
- (23) Frisch, M. J.; Trucks, G. W.; Schlegel, H. B.; Scuseria, G. E.; Robb, M. A.; Cheeseman, J. R.; Montgomery, J. A., Jr.; Vreven, T.; et al. *Gaussian 03*, revision C. 02; Gaussian, Inc.: Wallingford, CT, 2004.
- (24) Becke, A. D. Density Functional Thermochemistry. III. The Role of Exact Exchange. *J. Chem. Phys.* **1993**, 98, 5648.
- (25) Lee, C.; Yang, W.; Parr, R. G. Development of the Colle-Salvetti Correlation-energy Formula into a Functional of the Electron Density. *Phys. Rev. B* **1988**, 37, 785.
- (26) Mazalov, L.; Trubina, S.; Fomin, E.; Oglezneva, I.; Parygina, G.; Bausk, N.; Igumenov, I. X-Ray Study of the Electronic Structure of Copper(II) Acetylacetonate. *J. Struct. Chem.* **2004**, 45, 800–807.
- (27) Valli, M.; Matsuo, S.; Wakita, H.; Yamaguchi, T.; Nomura, M. Solvation of Copper(II) Ions in Liquid Ammonia. *Inorg. Chem.* **1996**, 35 (19), 5642–5645.
- (28) Sano, M.; Maruo, T.; Masuda, Y.; Yamatera, H. Structural Study of Copper(II) Sulfate Solution in Highly Concentrated Aqueous Ammonia by X-ray Absorption Spectra. *Inorg. Chem.* **1984**, 23, 4466–4469.
- (29) Mironov, V.; Pashkov, G.; Stupko, T. Thermodynamics of Formation Reaction and Hydrometallurgical Application of Metal–ammonia Complexes in Aqueous Solutions. *Russ. Chem. Rev.* **1992**, 61, 944.
- (30) Chaboy, J.; Muñoz-Páez, A.; Carrera, F.; Merklings, P.; Marcos, E. S. Ab Initio X-ray Absorption Study of Copper K-edge XANES Spectra in Cu(II) Compounds. *Phys. Rev. B* **2005**, 71, 134208.
- (31) Hennig, C.; Servaes, K.; Nockemann, P.; Van Hecke, K.; Van Meervelt, L.; Wouters, J.; Fluyt, L.; Görlner-Walrand, C.; Van Deun, R. Species Distribution and Coordination of Uranyl Chloro Complexes in Acetonitrile. *Inorg. Chem.* **2008**, 47, 2987–2993.
- (32) Rossberg, A.; Reich, T.; Bernhard, G. Complexation of Uranium (VI) with Protocatechuic Acid—Application of Iterative Transformation Factor Analysis to EXAFS Spectroscopy. *Anal. Bioanal. Chem.* **2003**, 376, 631–638.
- (33) Schwenk, C. F.; Rode, B. M. Cu<sup>II</sup> in Liquid Ammonia: An Approach by Hybrid Quantum-Mechanical/Molecular-Mechanical Molecular Dynamics Simulation. *ChemPhysChem* **2004**, 5, 342–348.
- (34) Pavelka, M.; Burda, J. V. Theoretical Description of Copper Cu(I)/Cu(II) Complexes in Mixed Ammine-Aqua Environment. DFT and ab initio quantum chemical study. *Chem. Phys.* **2005**, 312, 193–204.
- (35) Burda, J. V.; Pavelka, M.; Šimánek, M. Theoretical Model of Copper Cu(I)/Cu(II) hydration. DFT and Ab Initio Quantum Chemical Study. *J. Mol. Struct.-THEOCHEM.* **2004**, 683, 183–193.
- (36) Berces, A.; Nukada, T.; Margl, P.; Ziegler, T. Solvation of Cu<sup>2+</sup> in Water and Ammonia. Insight from Static and Dynamical Density Functional Theory. *J. Phys. Chem. A* **1999**, 103, 9693–9701.
- (37) Rao, K. S.; Sahoo, P. K. Effect of Ammonium Salts on the Extraction of Copper Using Hostarex DK-16. *Hydrometallurgy* **1993**, 33, 211–218.